Control-aware co-design of a wave energy converter for the Argentine sea conditions

1st Demián García-Violini*
Departamento de Ciencia y Tecnología
Universidad Nacional de Quilmes
Buenos Aires, Argentina
ddgv83@gmail.com

2nd Yerai Peña-Sanchez
Department of Mathematics
Euskal Herriko Unibertsitatea
Bizcaia, Spain
yerai.pena@ehu.eus

3rd Alejandro Otero
Centro de Simulación Computacional (CSC)
Universidad de Buenos Aires
CABA, Argentina
ddgv83@gmail.com

4th Roberto Sosa
INTECIN
Universidad de Buenos Aires
CABA, Argentina
rsosa@fi.uba.ar

5th Markel Penalba
Department of Fluid Mechanics
Mondragon University
Arrasate, Spain
mpenalba@mondragon.edu

6th John V. Ringwood
Centre for Ocean Energy Research (COER)
Maynooth University
Co. Kildare, Ireland
john.ringwood@mu.ie

2023 XX Workshop on Information Processing and Control (RPIC) | 979-8-3503-2941-4/23/$31.00 ©2023 IEEE | DOI: 10.1109/RPIC59053.2023.10530827

***Abstract*—Despite the favourable energy conditions in the Argentine sea (South Atlantic Ocean), the country has not yet actively participated in the development and utilisation of wave energy resources. Control co-design (CCD) is a novel control-aware design paradigm that integrates the energy-maximising control from early stages of system design, allowing for optimisation driven by the considered control strategy to achieve an overall optimal design. In this study, considering an overall control-aware design perspective, a wave energy converter system is specifically tailored for the Argentine sea conditions, analysing different WEC structural configurations (geometry and dimensions). The performance of different control structures, including a spectral-based control methodology and a reactive controller, are assessed for each configuration. Realistic operating conditions, specifically tailored to the ocean wave modes prevalent in the Argentine sea, are taken into account during the performance analysis. The results obtained from the study are thoroughly discussed, highlighting the advantages and disadvantages of the considered control strategies in the context of the Argentine sea.**

***Keywords*—Wave Energy, Control, Co-design, Argentina, Energy-Maximising Control**

I. Introduction

Ocean waves represent a considerable and untapped reservoir of renewable energy, with the potential to make a substantial contribution to global decarbonisation initiatives. Wave energy converters (WECs) have emerged as promising technologies for harnessing this resource, although their economic feasibility has not yet been fully established. In this regard, control system technology plays a critical role in optimising the energy absorption of WECs, addressing the inherent complexities involved in capturing and converting the irregular motion of ocean waves.

This work is supported by Agencia de I+D+i, under grant PICT-2021-I-INVI-00190.

*Demián García Violini (corresponding author), Alejandro Otero, and Roberto Sosa are also with CONICET, Argentina. In addition, Demián García-Violini is also with the Centre for Ocean Energy Research, Maynooth University, Ireland.

Although wave energy R & D have gained global momentum, Argentina has shown relatively less involvement in exploring this resource compared to its advancements in other non-carbon-based technologies, such as wind and solar power. However, recent developments indicate an increasing interest in wave energy within the country. Initiatives such as the "*Red de Energías Marinas Argentina*" (REMA) [1], events like the "*Encuentro Argentino de Energías Marinas 2022* (ENAEM 2022)" [2], and the international "*Wave Energy Workshop ENAEM-COER 2023*" [3], to be held in Buenos Aires in November 2023, along with a number of projects on wave energy financially supported by the "*Fondo Argentino Sectorial*" (FONARSEC), have raised awareness about the potential of wave energy in the country. In particular, it is worth noting that some of the project supported by the FONARSEC aim to develop and install full-scale WEC systems along the coast of Mar del Plata, Argentina, which represents a initial step in the development of WEC technologies in Argentina. Other noteworthy local developments in WEC technologies, with a particular focus on control, have been recently presented in the context of RPIC 2021 [4] and [5].

Recent advances in energy system design have introduced the concept of control co-design (CCD) [6], [7]. Traditional WEC design processes focus on optimising individual component specifications, such as absorber dimensions, geometrical shape, and power take-off (PTO). However, this fragmented approach may not lead to an overall optimal design. CCD addresses this challenge by integrating control strategy development into the early stages of WEC design, enabling general optimisation driven by the considered control strategy. This control-aware design paradigm aims to achieve an optimal structural design aligned with energy-maximising control schemes [8]–[11]. Although CCD implementation can be computationally demanding and restrictive, the literature explores three methodologies to address CCD challenges: (i) control-inspired paradigms, (ii) co-optimisation techniques,

and (iii) co-simulation methods [6]. Further details on these methodologies and CCD methods, in general, can be found in [6].

As mentioned before, maximising energy absorption from ocean waves is vital for the commercial competitiveness of WEC systems. Thus, control methodologies for WECs are categorised into optimisation-based (OB) and non-optimisation-based (nOB) approaches [12]. On the one hand, OB controllers, such as MPC, or those based on spectral-methods or moment-matching theory, solve the energy-maximising control problem as an optimal control problem (OCP). Thus, OB controllers, can effectively deal with constraints, providing (in theory) optimal solutions. However, OB methods are computationally demanding. On the other hand, nOB controllers, inspired by the impedance-matching principle, include, for example, the LiTe-Con method for broadband absorption, and reactive controllers (proportional-integral) for narrowband absorption. However, nOB methods cannot optimally deal with constraints.

The objective of this article is to present a control-aware design methodology, essentially inspired by control co-design (CCD) approaches, implemented using co-simulation methodologies. The design procedure considers both an OB controller, specifically a spectral-based controller [13], and a nOB controller, specifically a reactive controller. The WEC system under consideration is inspired by the technologies supported by the FONARSEC projects and consists of a rotational single degree-of-freedom (DoF) system with a hemispherical buoy and a rotational arm. Various arm lengths and a wide range of radii are explored in the WEC design. This design methodology offers a comprehensive perspective that aligns with current design trends, incorporating an optimal controller capable of handling constraints and a resistive-reactive controller, widely considered in the literature and industry of WEC systems.

The subsequent sections of this work are structured as follows. Section II recalls the fundamentals of WEC modelling. In Section III, the control approaches considered for this study are discussed. Section IV introduces the presented control-aware design technique. A case study is provided in Section V, featuring the application of the technique to a generic, full-scale, and realistic WEC system. Finally, Section VI serves as the conclusion of this work, providing a summary of key findings and a discussion of the implications of the presented approach.

II. WEC Modelling Framework

In the context of WEC systems in an undisturbed wave field and an infinite-depth sea, fluid-structure interactions are accounted for using potential flow theory. The fluid is assumed to be inviscid, incompressible, and irrotational. By applying Newton's second law to a rotational-type single DoF[1] WEC device, a linear hydrodynamic formulation is derived as follows [14]:

$$(I + A_\infty)\,\ddot{\theta}(t) + \tau_{\mathrm{r}}(t) + \tau_{\mathrm{h}}(t) = \tau(t) - \tau_{\mathrm{u}}(t), \qquad (1)$$

which is defined in the literature as Cummins' equation, a well-established and widely adopted theoretical framework [15]. In Eq. (1), the angular acceleration, and, implicitly, velocity and position, of the device are represented by $\ddot{\theta}(t)$, $\dot{\theta}(t)$, and $\theta(t)$, respectively, with I indicating the body inertia and A_∞ the added mass at infinite frequency [14]. The radiation torque, denoted as $\tau_{\mathrm{r}}(t)$, is defined as the convolution integral of the radiation torque impulse response $h_{\mathrm{r}}(t)$ with the angular velocity $\dot{\theta}(t)$, i.e. $\tau_{\mathrm{r}}(t) = h_{\mathrm{r}}(t) * \dot{\theta}(t)$. The restoring torque, representing buoyancy, is expressed as $\tau_{\mathrm{h}}(t) = s_{\mathrm{h}}\theta(t)$, where s_{h} represents hydrostatic stiffness. Additionally, the control torque applied through the PTO system is denoted as $\tau_{\mathrm{u}}(t)$, while $\tau(t)$ represents the excitation torque, which is generated by the action of the surrounding waves.

Considering the well-established Ogilvie's relations [16], the system in Eq. (1), can be redefined in the Laplace domain, as follows:

$$G(s) = \frac{s}{s^2(I + A_\infty) + s\hat{H}_{\mathrm{r}}(s) + s_{\mathrm{h}}}, \qquad (2)$$

which is the so-called torque-to-motion mapping, where $\hat{H}_{\mathrm{r}}(s)$ is an approximated parametric representation of $H_{\mathrm{r}}(\omega)$ for $s = \jmath\omega$, with $H_{\mathrm{r}}(\omega)$ the Fourier transform of $h_{\mathrm{r}}(t)$. In particular, $h_{\mathrm{r}}(t)$ ($H_{\mathrm{r}}(\omega)$) is typically obtained using boundary-element methods, such as NEMOH [17], while the approximation $\hat{H}_{\mathrm{r}}(s)$ can be obtained with system ID parameter fitting tools [18].

A. Control Objective

The primary objective in the control of WECs is to maximise the total absorbed energy. For a WEC system, which experiences an external excitation torque $\tau(t)$, while controlled by the action of the PTO system, the total absorbed energy over the interval $[0, T]$ is determined as follows[2]:

$$E = -\int_0^T P(t)dt = -\int_0^T \dot{\theta}(t)^{\intercal}\tau_{\mathrm{u}}(t)dt, \qquad (3)$$

where $P(t)$ represents the instantaneous power, and $\tau_{\mathrm{u}}(t)$ and $\dot{\theta}(t)$ are introduced in Eq. (1). In Eq. (3), the transpose operator is consistent with multi DoF, and within the context of this study, it is particularly aligned with spectral methods, as discussed in Section III-B. Thus, the control problem can be defined as follows:

$$\begin{aligned} \max_{\tau_{\mathrm{u}}(t)} \quad & -\int_0^T \dot{\theta}(t)^{\intercal}\tau_{\mathrm{u}}(t)dt \\ \text{subject to} \quad & \begin{cases} \dot{\mathrm{x}} = \mathcal{F}(\mathrm{x}, \tau_{\mathrm{u}}, \tau) \\ \dot{\theta} = \mathcal{G}(\mathrm{x}) \\ \mathcal{C} \end{cases} \end{aligned} \qquad (4)$$

where $\mathcal{F}(x, \tau_{\mathrm{u}}, \tau)$ denotes the state-space representation of the system in Eq. (1), $\mathcal{G}(\mathrm{x})$ the output mapping $\mathrm{x} \mapsto \dot{\theta}$, and $\mathcal{C}$ a general set of constraints (such as displacement constraints $\theta_{min} \leq \theta(t) \leq \theta_{max}$, or PTO torque constraints $\tau_{\mathrm{u}_{min}} \leq \tau_{\mathrm{u}}(t) \leq \tau_{\mathrm{u}_{max}}$, etc.), specifically defined for each WEC control problem.

[1] Without loss of generality. The same discussion can be easily extended to multiple DoF.

[2] From now on, the time dependence is dropped when clear from the context.

B. Optimal condition in the frequency domain

Considering the torque-to-velocity mapping in Eq. (2), an alternative approach to address the control problem is based on the impedance-matching condition for achieving maximum power transfer [14]. Specifically, let $Z = G(\jmath\omega)^{-1}$ the intrinsic impedance of the WEC system. It can be shown that the optimal control law, which maximises Eq. (3) under linear modelling assumptions, can be characterised in the frequency domain as:

$$\mathcal{T}(\jmath\omega) = Z^{\star}(\jmath\omega)\dot{\Theta}(\jmath\omega), \tag{5}$$

where the symbol $\star$ denotes the complex conjugate operator, while the symbol $\dot{\Theta}(\jmath\omega)$ denotes the Fourier transform of the angular velocity $\dot{\theta}(t)$. However, a challenge arises due to the anticausal behaviour exhibited by $Z^{\star}$, as a consequence of the features of $G(s)$, i.e. strictly proper and passive. A family of controllers, including the impedance-matching-based solutions discussed in Sections III, aim to find a causal controller, typically LTI, that approximates condition in Eq (5) in a suitable manner. It is worth noting that while this approach leads to simple and easily implementable controllers, they tend to be suboptimal compared to those specifically designed to solve Eq (4).

III. Controllers

A. Reactive control

The widely-used reactive, which can be considered as PI, controller is a standard feedback energy-maximising control solution in the WEC literature. It calculates the control torque as a linear combination of position and velocity:

$$\tau_u(t) = \begin{bmatrix} k_\theta & k_{\dot{\theta}} \end{bmatrix} \begin{bmatrix} \theta(t) \\ \dot{\theta}(t) \end{bmatrix}, \tag{6}$$

which, in terms of the Laplace domain, can be expressed as:

$$\mathcal{T}_u(s) = \frac{k_\theta s + k_{\dot{\theta}}}{s}\dot{\Theta}(s). \tag{7}$$

Based on the impedance-matching condition discussed in Section II-B, analytical conditions can be derived to maximise absorbed energy *with monochromatic waves*. Consequently, the parameters for the reactive PI controller can be computed as follows:

$$k_\theta = \mathbb{R}\mathrm{e}\left\{\Gamma(\omega^*)\right\}, \quad k_{\dot{\theta}} = -\omega^* \mathbb{I}\mathrm{m}\left\{\Gamma(\omega^*)\right\}, \tag{8}$$

where

$$\Gamma(\omega^*) = \frac{1}{T^{\alpha}_{\tau\mapsto\dot{\theta}}(\omega^*)} - \frac{1}{G(\jmath\omega^*)}, \tag{9}$$

and ω^* represents a specific frequency targeted for maximising energy absorption, while $T^{\alpha}_{\tau\mapsto\dot{\theta}}(\omega^*)$ corresponds to the resulting torque-to-velocity mapping obtained with the optimal condition, introduce for Eq (5) [19], modified with α to achieve constraint handling. In particular, the mapping in Eq. (5), can be explicitly defined as

$$T^{\alpha}_{\tau\mapsto\dot{\theta}}(\omega^*) = \alpha\frac{\mathbb{R}\mathrm{e}\left\{G(\jmath\omega^{\star})\right\}^2 + \mathbb{I}\mathrm{m}\left\{G(\jmath\omega^{\star})\right\}^2}{2\mathbb{R}\mathrm{e}\left\{G(\jmath\omega^{\star})\right\}}, \tag{10}$$

where $\alpha \in [0,\, 1]$ is used to handle motion constraints. In particular, if $\alpha = 1$ the optimal condition, given for the unconstrained case by the impedance-matching principle, is obtained while, if $\alpha = 0$, the system is absolutely blocked (no motion). Consequently, in the unconstrained case, the impedance-matching condition is satisfied at ω^*. Nevertheless, for the unconstrained case, the essential condition for energy-maximisation, described by zero-phase locking in Eq. (10), is guaranteed (see [19]).

B. Spectral control

Spectral control is an approach that employs spectral methods for the analysis and design of control systems [13]. Spectral methods involve approximating functions using specific sets of basis functions, such as Fourier, Legendre, or Chebyshev polynomials [13]. To apply spectral control to WEC systems (see, for example, [13]), the optimal control formulation in Eq. (4) is discretised in the spectral domain by projecting x and τ_{u} onto a vector space of dimension N_{sp} using a linear combination of orthogonal basis functions denoted as $\Phi = \{\phi_i\}_{i=1}^{N_{sp}}$. The Fourier basis functions can be used for this purpose, i.e. $\Phi = \left[\sin(w_1 t),\, \cos(w_1 t),\, \ldots,\, \sin(\frac{\omega_{N_{sp}}}{2}t),\, \cos(\frac{\omega_{N_{sp}}}{2}t)\right]$. Consequently, the states and control torque are approximated as follows:

$$x_i(t) \approx x_i^{N_{sp}}(t) = \Phi^{\intercal}(t)\hat{\mathrm{x}}_i, \quad \tau_{\mathrm{u}}(t) \approx \tau_{\mathrm{u}}^{N_{sp}}(t) = \Phi^{\intercal}(t)\hat{\tau}_{\mathrm{u}}, \tag{11}$$

where coefficient vectors are defined as $\hat{x}_i = [x_{i1} \cdots x_{iN_{sp}}]^{\intercal}$, and $\hat{\tau}_{\mathrm{u}} = [\tau_{\mathrm{u}1}, , \cdots \tau_{\mathrm{u}Nsp}]^{\intercal}$, both in $\mathbb{R}^{N_{sp}}$. Within the framework of this spectral approach, an approximation for the equation of motion can be expressed as [13]:

$$\hat{\dot{\theta}} = \mathrm{G_o}(\hat{\tau} - \hat{\tau}_{\mathrm{u}}), \tag{12}$$

where $\hat{\dot{\theta}} = [\dot{\theta}_1\ \dot{\theta}_2\ \cdots\ \dot{\theta}_{Nsp}]^{\intercal}$ represents the coefficient vector used to approximate the angular velocity $\dot{\theta}(t)$ of the system, while $\mathrm{G_o}$ denotes the torque-to-velocity system *model* (block diagonal matrix) as described in [13]. Furthermore, in Eq. (12), $\hat{\tau} = [\tau_1, , \cdots\ \tau_{Nsp}]^{\intercal} \in \mathbb{R}^{N_{sp}}$, where the set $\{\tau_i\}_{i=1}^{N_{sp}}$ contains the coefficients of the excitation torque approximation.

The main goal of the optimal control problem is to determine the control torque $\tau_{\mathrm{u}}(t)$ that maximises the objective function presented in Eq. (3), while satisfying the equation of motion. Leveraging the mathematical properties of the basis functions Φ_j [20], the objective function in Eq. (3) can be approximated as:

$$E \approx J_N = \int_0^T \hat{\tau}_{\mathrm{u}}^{\intercal}\Phi^{\intercal}(t)\Phi(t)\hat{\dot{\theta}}dt = -\frac{T}{2}\hat{\tau}_{\mathrm{u}}^{\intercal}\hat{\dot{\theta}}, \tag{13}$$

By employing Eqs.(12) and (13), the objective function can be rewritten as:

$$J_N = -\frac{T}{2}\hat{\tau}_{\mathrm{u}}^{\intercal}\mathrm{G_o}(\hat{\tau} - \hat{\tau}_{\mathrm{u}}). \tag{14}$$

1) General optimal solution: Constrained and unconstrained cases

Considering spectral methods, the control problem for WEC systems can be formulated as follows:

$$\begin{aligned} \hat{\tau}_{\mathrm{u}}^{\star} \leftarrow \max_{\hat{\tau}_{\mathrm{u}} \in \mathbb{R}^N} \quad & J_N \\ \text{subject to:} \quad & \mathcal{C}, \end{aligned} \tag{15}$$

with $\hat{\tau}_{\mathrm{u}}$ the control torque vector to be optimised, and $\mathcal{C}$ represents a set of constraints based on the physical limita-

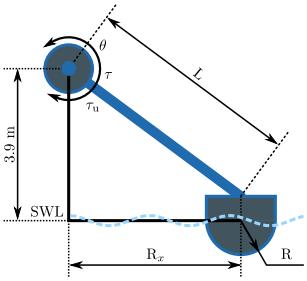

Fig. 1. Considered WEC structure. It is based on a rotational single DoF system, comprising a hemispherical buoy and a rotational arm.

tions of the WEC system. The constraints can include, for example, maximum device displacement (Θ_{max}) or maximum PTO torque ($\mathcal{T}_{\text{max}}$). Generally, the optimisation problem in Eq. (15) can be solved by satisfying the constraints at specific collocation points ($\mathbf{T}_c = [t_1, t_2, \ldots, t_{N_c}]$). A comprehensive discussion on defining a set of linear inequalities required to satisfy constraints at collocation points can be found in [21].

By employing collocation points, standard multipurpose optimisation solvers, such as QP-problem solvers, can be utilised to tackle the problem presented in Eq. (15) [22].

IV. Control-aware design

This section provides an overview of the design methodology considered in this study. The considered WEC structure is based on a rotational single DoF system, comprising a hemispherical buoy and a rotational arm, as illustrated in Fig. 1. The design procedure follows a parametric scheme, with the key design variables being R, representing the radius of the buoy, and R_x, indicating the horizontal distance to the pivot point. Furthermore, Fig. 1 presents the main variables involved in the design process, including τ, τ_{u}, and θ. Importantly, the vertical distance to the pivot point has been considered constant at 3.9 m throughout this study (as indicated in Fig. 1), a decision that is explained in more detail in Section V. On the other hand, the horizontal distance is considered a variable design parameter. It is worth noting that this study is motivated by projects financed by the FONARSEC, which involve the installation and operation of WECs, similar to the one depicted in Fig. 1, along the coast of Mar del Plata, Argentina, as mentioned in Section I.

To achieve an control-aware optimal design, the principal optimisation problem is expressed as follows:

$$\begin{aligned} \rho^\star \leftarrow \quad & \min_{\rho \in \Psi \subset \mathbb{R}^N_\rho} && f \\ & \text{subject to:} && \text{Solve Eq. (15)} \\ & && \mathcal{C}, \end{aligned} \tag{16}$$

where $\rho \in \Psi \subset \mathbb{R}^{N_\rho}$ denotes the design parameter vector. As an illustration, considering the configuration depicted in Fig. 1, the vector ρ is given by $[R, R_x]^\intercal$. Additionally, in Eq. (16), the objective function f is defined based on the specific design requirements pertinent to each individual problem. For instance, one possible criterion is the total WEC cost, encompassing both capital and operational expenditures (CapEx and OpEx), per unit of absorbed power, as explored in [21]. Another potential consideration is the total buoy mass per unit of absorbed power. The buoy mass significantly impacts the CapEx and is directly proportional to the installation cost of the system. Therefore, the objective function in Eq. (16), is given by:

$$f = AP(\rho)/M(\rho), \tag{17}$$

In Eq. (17) $AP(\rho)$ indicates the total (average) absorbed power, obtained from Eq. (3). In this study, the optimisation problem introduced in Eq. (16) is solved using a exhaustive search search methodology. However, it must be noted that Eq. (16) can be addressed using, for example, multi-objective optimisation routines [23]. Nevertheless, employing a brute-force approach, akin to a parametric study, offers distinct benefits as it comprehensively explores all potential scenarios, effectively highlighting the intricate interactions among parameters. This deeper understanding of the problem and solution domains is a direct result of examining the complete range of possibilities.

V. Illustrative Example

A. WEC system

The considered device is a point-absorber type, with an axis-symmetric cylindrical geometry, and a hemispherical bottom, as depicted in Fig 1. For this study, the principal design variables are given by the radius, R, and the horizontal distance, R_x, from the buoy to the pivot point. To ensure that the relationship between R and R_x remains within realistic bounds, the horizontal distance is considered as a linear function of R, as follows:

$$R_x = \ell R, \text{ with } \ell \in [2,\, 6]\,, \text{ and } R \in [0.5,\, 10]\,. \tag{18}$$

With these definitions, the hydrodynamical coefficients are calculated for each system in a grid. NEMOH [17] is used for this purpose, considering a mesh as illustrated in Fig. 2. The grid is

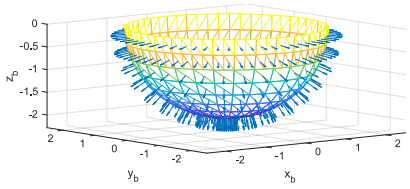

Fig. 2. Mesh considered for each system defined in Eq. (18) (submerged structure).

defined for intervals specified in Eq. (18), with increments of 0.5 m, for both R and R_x. For each combination of R and R_x, the hydrodynamic coefficients are computed using NEMOH. The resulting torque-to-velocity (angular) frequency response is depicted in Fig. 3 for specific cases of $R \in \{2, 5, 10\}$ m. The responses in Fig. 3 are represented using coloured groups of lines, with a colour gradient indicating the corresponding values of ℓ. Fig. 3 provides a clear visualisation of the progression of both the resonance frequency and attenuation level.

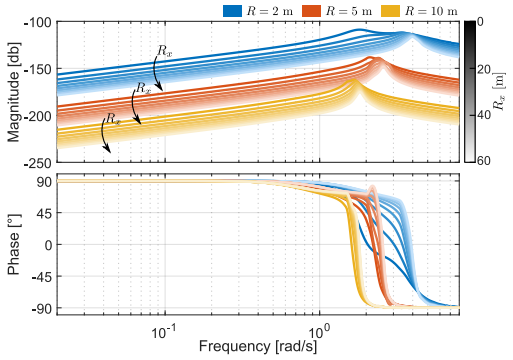

Fig. 3. Torque-to-velocity (angular) frequency response for specific cases of $R \in \{2, 5, 10\}$. The variation of ℓ is indicated with the generic colour gradient (grey scale), illustrated on the right-hand-side.

In each simulation, the angular position is constrained to $\Theta_{\text{max}} = 30°$, 0.523 rad, symmetric, (pivot point in Fig. 1), to preserve a realistic rotational motion. In addition, full knowledge (*a-priori*) of the wave excitation force is considered in this study. The simulation length is set to 200 s.

B. Sea states

As considered and described in [5], based on the studies presented in [24], a sea-state with peak period $T_p = 10$ s and significant wave height $H_s = 2$, characterised by the so-called JONSWAP spectrum (see [25]), is considered in this study, with the so-called peak-enhancement factor set to 3.3 [5]. This sea description has been taken for the global position at $38°03'25.035''$ S, $57°29'24.201''$ W. These parameters have been also supported by the results in [26]. However, the reader must note that there are no accurate and formal information about the sea conditions in the South Atlantic Ocean available in the literature. Thus, one of the objective of the projects supported by the FONARSEC is to develop precise models for the Argentine sea conditions. For statistical consistency, the results are averaged over 10 random realisations.

C. Controller design

The PI control structure discussed in Section III-A is firstly addressed in this section. For each simulation the controller is tuned considering $w^\star = \frac{2\pi}{T_p}$. To ensure respect of the constraint limits, Θ_{max}, the parameter α, in Eq. (10), is individually tuned for each realisation. Hence, the controller parameters, k_θ and $k_{\dot\theta}$, as defined in Eq. (9), are determined for each simulation.

Secondly, in the spectral control scheme, a collection of Fourier basis functions is employed, consisting of $N_{sp} = 67$ basis functions. To effectively cover the wave spectrum, these basis functions cover a range of frequencies spanning from $0.7\omega^\star$ to $4\omega^\star$ in steps of $0.05 \times \frac{2\pi}{T_w}$. In addition, motion constraints are considered to fulfil the constraints defined by P_{lim}. The resulting (concave) QP-problem is solved via interior-point methods [22].

D. Control-aware design: Results and assessment

For the assessment of introduced control-aware methodology, the objective function for the optimisation problem considered in Eq. (16), is considered as follows:

$$f = \frac{AP(\rho)}{M(\rho) + w_L L(\rho)} \tag{19}$$

where $\rho = [R,\, R_x]$, M denotes the mass of the buoy, which depends on R, and L represents the linear distance to the pivot point (see Fig. 1), which depends on R_x along with the fixed vertical distance (3.9 m for this study). Please note that the expression in Eq. (19) broadly represents 1/LCoE (levelised cost of energy), i.e. power production/cost, which is to be maximised (see [21]). In addition, w_L is a fixed weighting variable to simultaneously assess the mass and the length of the WEC. Specifically, in this study, the value of w_L is set to 7000. It must be noted that, while the parameter w_L is empirically tuned in this study for the general purpose of demonstrating how structural design can influence the optimum design point, the distance L can directly impact the CapEx. Specifically, a greater distance from the lever arm leads to increased stresses in the anchoring system of the pivot structure. This, in turn, results in higher costs associated with the installation and maintenance of the system.

Fig. 4(a) displays the average absorbed power for both the spectral and PI control methodologies, with the spectral control shown in orange-light scale and the PI control depicted in greyscale, for the complete domain Ψ. Similarly, using the same colour code, Fig. 4(b) shows the resulting (normalised to one) value of the objective function f, in Eq. (19).

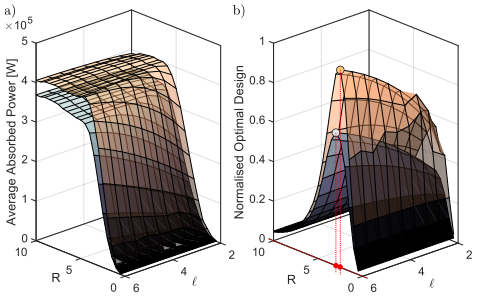

Fig. 4. The average absorbed power and the normalised resulting value of f is shown in (a) and (b), respectively. In (b) the optimal point obtained with each control structure is shown using a red dot.

In Fig. 4(b), the optimal points obtained with each control structure (spectral and PI) are depicted by red dots. Notably, from Fig. 4, it is evident that in both cases, the optimal point is achieved with $\ell = 6$. However, the optimal values for R are different, with 2.5 m and 3 m attained for the spectral and PI control, respectively. Notably, this optimal results do not match the point of maximum power absorption (Fig. 4(a)), which are given by the largest values of R and ℓ (R_x). This emphasises the importance of employing a global optimisation criterion rather than relying solely on a conventional energy absorption approach.

By way of example, Fig. 5 shows both τ_u and τ (a), along with the vertical position (b) and velocity (c), for a particular realisation of the considered sea-state, for each optimal solution (red dots in Fig. 4), confirming that both controllers are adhering to the specified constraints.

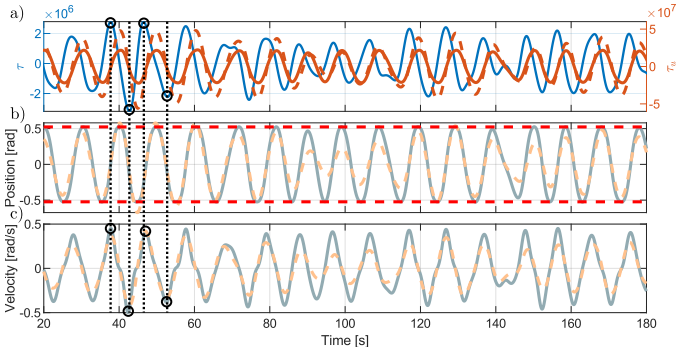

Fig. 5. (a) Time traces for τ_u (blue-solid line) and τ (grey and pink lines). (b) Time traces for the vertical position. The considered limit $\Theta_{\max} = 30°$, 0.523 rad, symmetric, is indicated with red-dashed line.

Additionally, Fig. 5 visually demonstrates the effectiveness of each control methodology, for the optimal solutions shown in Fig. 4. In particular, the synchronisation between the excitation torque (a) and the system velocity (c) at four specific times, which represents a key indicator of effectiveness. Circular empty markers and dotted lines are used to represent these instances. In addition, in Fig. 5(b) the vertical position limits of the system is shown, using red-dotted lines, which shows the constraint fulfilment obtained with each control methodology.

VI. Conclusion

This work explores the relationship between the structural design of a specific WEC system and its energy maximisation control problem, guided by the design criterion f. While some simplifying assumptions are made, a more comprehensive economic model could enhance the process. Despite these simplifications, the nonlinearity of the design parameters (R and R_x) leads to a challenging optimisation problem. This study underscores the significance of utilising a global optimisation criterion instead of exclusively depending on a conventional energy absorption strategy. Employing an exhaustive search approach, a parametric study reveals various parameter configurations, emphasising the importance of informed choices for optimising WEC performance. Moreover, this study lays the foundation for designing a full-scale WEC system tailored for the Argentine sea. The insights gained will be crucial in harnessing the energy potential in the South Atlantic Ocean, contributing to wave energy resource utilisation. Additionally, for the final WEC installation, essential aspects like the anchor system, grid connection, and security considerations must be taken into account to ensure successful and safe implementation in its actual operating environment.

References

[1] Red de Energías Marinas Argentina (REMA), "REMA website," https://www.redenergiasmarinas.ar/, 2023, [Online accessed 1-Jul-2023].

[2] Encuentro Argentino de Energías Marinas 2022 (ENAEM2022), "ENAEM 2022 website," https://www.redenergiasmarinas.ar/enaem-2022, 2023, [Online accessed 1-Jul-2023].

[3] Wave Energy Workshop 2023 ENAEM-COER 2023, "ENAEM-COER 2023 website," enaemcoer2023.ar, 2023, [Online accessed 1-Jul-2023].

[4] D. García-Violini, M. Farajvand, C. Windt, V. Grazioso, and J. V. Ringwood, "Passivity considerations in robust spectral-based controllers for wave energy converters," in *2021 XIX Workshop on Information Processing and Control (RPIC)*, 2021, pp. 1–6.

[5] N. Faedo, D. García-Violini, Y. Peña-Sanchez, and J. V. Ringwood, "On the feasibility of energy-maximising controllers for an argentinian wave energy system," in *2021 XIX Workshop on Information Processing and Control (RPIC)*, 2021, pp. 1–6.

[6] M. Garcia-Sanz, "Control co-design: an engineering game changer," *Advanced Control for Applications: Engineering and Industrial Systems*, vol. 1, no. 1, p. e18, 2019.

[7] A. Alleyne, F. Allgöwer, A. Ames, S. Amin, J. Anderson, A. Annaswamy, P. Antsaklis, N. Bagheri, H. Balakrishnan, B. Bamieh *et al.*, "Control for societal-scale challenges: Road map 2030," in *2022 IEEE CSS Workshop on Control for Societal-Scale Challenges*. IEEE Control Systems Society, 2023.

[8] P. B. Garcia-Rosa, G. Bacelli, and J. V. Ringwood, "Control-informed optimal array layout for wave farms," *IEEE Transactions on Sustainable Energy*, vol. 6, no. 2, pp. 575–582, 2015.

[9] M. Neshat, B. Alexander, N. Y. Sergiienko, and M. Wagner, "A hybrid evolutionary algorithm framework for optimising power take off and placements of wave energy converters," in *Proceedings of the Genetic and Evolutionary Computation Conference*, 2019, pp. 1293–1301.

[10] P. B. Garcia-Rosa and J. V. Ringwood, "On the sensitivity of optimal wave energy device geometry to the energy maximizing control system," *IEEE Transactions on Sustainable Energy*, vol. 7, no. 1, pp. 419–426, 2015.

[11] R. G. Coe, G. Bacelli, S. Olson, V. S. Neary, and M. B. R. Topper, "Initial conceptual demonstration of control co-design for wec optimization," *Journal of Ocean Engineering and Marine Energy*, vol. 6, no. 4, pp. 441–449, 2020. [Online]. Available: https://doi.org/10.1007/s40722-020-00181-9

[12] N. Faedo, D. García-Violini, Y. Peña-Sanchez, and J. V. Ringwood, "Optimisation-vs. non-optimisation-based energy-maximising control for wave energy converters: A case study," in *2020 European Control Conference (ECC)*, 2020, pp. 843–848.

[13] D. Garcia-Violini and J. V. Ringwood, "Energy maximising robust control for spectral and pseudospectral methods with application to wave energy systems," *International Journal of Control*, vol. 94, no. 4, pp. 1102–1113, 2021.

[14] J. Falnes, *Ocean waves and oscillating systems: linear interactions including wave-energy extraction*. Cambridge Univ. Press, 2002.

[15] W. E. Cummins, "The impulse response function and ship motions," *Schiffstechnik*, vol. 47, pp. 101–109, 1962.

[16] T. F. Ogilvie, "Recent progress toward the understanding and prediction of ship motions," in *5th Symposium on Naval Hydrodynamics*, vol. 1. Bergen, Norway, 1964, pp. 2–5.

[17] LHEEA, NEMOH-Presentation, "Laboratoire de Recherche en Hydrodynamique Énergetique et Environnement Atmospherique," https://goo.gl/yX8nFu, 2017, [Online accessed 1-Jul-2023].

[18] L. Ljung, *System Identification - Theory for the User*. Prentice Hall, 1999.

[19] D. García-Violini, Y. Peña-Sanchez, N. Faedo, and J. V. Ringwood, "An energy-maximising linear time invariant controller (LiTe-Con) for wave energy devices," *IEEE Transactions on Sustainable Energy*, vol. 11, no. 4, pp. 2713–2721, 2020.

[20] D. García-Violini, M. Farajvand, C. Windt, V. Grazioso, and J. V. Ringwood, "Passivity considerations in robust spectral-based controllers for wave energy converters," in *2021 XIX Workshop on Information Processing and Control (RPIC)*. IEEE, 2021, pp. 1–6.

[21] Y. Peña-Sanchez, D. García-Violini, and J. V. Ringwood, "Control co-design of power take-off parameters for wave energy systems," *IFAC-PapersOnLine*, vol. 55, no. 27, pp. 311–316, 2022.

[22] The MathWorks, Inc., *MATLAB Optimization Toolbox*, The MathWorks, Inc., Release Year. [Online]. Available: https://www.mathworks.com/products/optimization.html

[23] K. Miettinen, *Nonlinear multiobjective optimization*. Springer Science & Business Media, 2012, vol. 12.

[24] C. K. Parise and L. Farina, "Ocean wave modes in the south atlantic by a short-scale simulation," *Tellus A: Dynamic Meteorology and Oceanography*, vol. 64, no. 1, p. 17362, 2012.

[25] K. Hasselmann, "Measurements of wind wave growth and swell decay during the Joint North Sea Wave Project (JONSWAP)," *Deutches Hydrographisches Institut*, vol. 8, p. 95, 1973.

[26] B. E. Prario and W. C. Dragani, "Clima de olas: análisis del recurso en sitios costeros de Mar del Plata, Argentina. Servicio de Hidrografía Naval (SHN)." in *Proceedings of the Encuentro Argentino de Energías Marinas 2022 (ENAEM 2022)*, 2022, pp. 1–6.